Quantitative evaluation of stereoscopic augmented reality visualization using an optical see-through head-mounted display

MAGDALENA ŻUK*, MARCIN MAJAK, IZABELA SZCZUR,
MICHAŁ POPEK, EWELINA ŚWIĄTEK-NAJWER

Faculty of Mechanical Engineering, Department of Mechanics, Material and Biomedical Engineering,
Wrocław University of Science and Technology, Wrocław, Poland.

Purpose: The authors of the current study aimed to propose a calibration method for accurate augmented reality visualisation using an optical see-through head-mounted display, and to qualitatively evaluate visualisation accuracy for the application in computer assisted surgery. *Methods*: An adaptation of stereo single-point active alignment method was proposed as the calibration procedure together with verification. Three tests were performed: display of points in 3D space, on the plane and on the surface of a skull phantom on inexperience users (5 participants) and experienced users (17 participants). *Results*: The highest accuracy of visualization was obtained for skull phantom visualisation for an inexperienced user (3.00 mm, std 0.75 mm), while the lowest accuracy was obtained in a 3D visualisation test for an inexperienced user (22.95 mm, std 18.04 mm). The largest error was related to the depth component and amounted to 18.49 mm, std 18.10 mm for an inexperienced user. *Conclusions*: It is possible to achieve relatively high visualisation accuracy (less than 5 mm for visualisation in space) for selected users but providing it for the group of inexperienced users seems to remain a major challenge. The accuracy of point indication can be substantially and statistically significantly increased by visualising objects on surfaces. The proposed methods and obtained results can serve as a basis for further implementation of augmented reality visualisation on an optical see-through head-mounted display in applications requiring high-quality augmented reality guidance of manual tasks.

Key words: *augmented reality, optical a see-through head-mounted display, computer aided surgery, single point active aliment method*

1. Introduction

Augmented reality (AR) is a technology that blends virtual objects with real environments [1]. This technology has been widely disseminated in the form of apps for smartphones and tablets and does not require the user to use dedicated devices. At the same time, recent years have seen the development and emergence on the market of various wearable AR devices, referred to as head-mounted displays (HMDs). These devices display an image directly in front of the user's eyes, thus providing an egocentric viewpoint that allows the user to work hands-free. This solution expands the applicability of this technology, including domestic and industrial applications where graphical information is required in real time, in such areas as entertainment and gaming, medicine and telemedicine, engineering, manufacturing, automotive and architecture. A distinction can be made between devices in which virtual objects are superimposed on the camera image (video see-through HMDs) and devices showing the real image (optical see-through HMDs) [1]. An optical see-through (OST) HMD is a device that

projects virtual images directly in front of the user's yes and allows the user to see the real world through them. OST HMDs use optical devices such as a half-silvered mirror or beam splitter to merge the real view and virtual content from micro-displays installed in the HMD frame outside the see-through screen [2]. Currently, this real-time interactive technology is developing rapidly largely due to an increase in the number commercially available, consumer-oriented devices such as the Epson Moverio series (BT-200 and BT-300, Seiko Epson Corp., Japan), Microsoft Hololens 2 (Microsoft Corp., USA) and Vuzix series (Vuzix Corp., USA).

An important aspect of OST AR technology is the visualisation of virtual objects superimposed on the real image. In its most advanced form, such a visualisation is a form of extension of the sense of sight, where a computer generated 3D object is displayed in a preset position in space (stereoscopic vision) while perfectly blending in with the real image (correctly handling the occlusion effect). The implementation requires, first of all, mastering the accurate visualisation of virtual objects at a preset position in space. The next step involves the use of space mapping methods to represent the occlusion effect correctly. This study focuses on the first aspect: visualisation of spatial objects in a preset position in space. A particular challenge is the visualisation itself, but also an assessment of its accuracy, which is related to subjective perception of vision, individual differences and lack of direct preview of the user's view in the OST technology (as opposed to the video see-through technology). In order to render the perceived virtual objects as spatially aligned with the physical environment, it is also necessary to accurately measure the position of the OST HMD and the position of the user's eyes [3]. While measuring the position of the OST HMD is simpler to implement and comes down to using an external or embedded six-degrees-of-freedom tracking system, determining the position of the user's eyes is much more challenging and requires the use of a calibration method. Several calibration methods have been proposed in previous studies. Grubert et al. [3] provided an overview of calibration procedures, classifying them into manual, semi-automatic and automatic approaches. Manual calibration methods require the human operator to provide 3D–2D correspondences by manually aligning 3D world objects with 2D points displayed on the see-through HMD screen and a computer monitor screen. This study focuses on adaptations of a variant of the single point active alignment method (SPAAM) proposed by Tuceryan at al. [4] SPAAM involves repeatedly aligning a single point displayed

on a monocular OST HMD screen (optical combiner/splitter) with a point in the real world. In this method, at least six 2D–3D correspondences are used to create and solve linear equation according to the DLT method [3], [4] and consequently obtain the projection matrix. An advantage of this method is its low hardware requirements: apart from an OST HMD, it only requires a tracking system, so this solution can be used in many applications. Ensuring high accuracy for the SPAAM method requires separate registration for each user, preferably each time the OST HMD is put on, and collection of calibration points at several depths corre-sponding to the target workspace. Genc et al. [5] proposed a two-stage SPAAM (SPAAM2), where the original calibration was used and only some of the parameters were re-estimated based on just two 2D–3D correspondence points. Genc et al. [6] extended the SPAAM method to stereo display calibration, which involved aligning a virtual 3D object projected in a binocular OST HMD (by displaying the object on both displays with some disparity) with a 3D object in the real world. Grubert et al. [3] proposed the multiple point active alignment method (MPAAM), where a grid of nine 3D points is simultaneously aligned on the calibration board by the user. Zhang et al. [7] proposed a calibration framework, including SPAAM calibration according to Tuceryan et al. [4] and integration of a depth camera as an alternative to the navigation system. Most of the studies concern increasing the user-friendliness of the SPAAM implementation, since users may find it too time-consuming and workload-intensive. Such changes may enable the users to carry out a single calibration, which can then be used in subsequent sessions [3]. Another important aspect is to ensure the accuracy of the visualization, which determines the areas of application. Evaluation is especially challenging in the case of an OST HMD because there is no way to access the augmented image on the user's retina – only the user can see it. Therefore, the traditional image-based method of assessing accuracy cannot be applied in this case. Different SPAAM variants have been evaluated in previous papers [7]–[11]. McGarrity et al. [12] proposed a method of quantifying the geometric error. However, most studies report reprojection errors in pixels, making it difficult to compare different methods due to the different HMD resolutions and distances between the user's eyes and the virtual screen [3]. A promising area of AR application using an OST HMD is medicine [13], including computer-assisted surgery (CAS) for accurate visualization of anatomical data and a preoperative virtual plan to increase the ergonomics of the surgeon's work while maintaining the accuracy of

the procedure. Moreover, the use of an OST HMD may possibly improve depth perception in minimal invasive surgery [14]. An advantage of using an OST HMD in CAS is that the surgeon does not need to look at an external monitor and can maintain the line of sight with the surgical field. In addition, spatial visualization with binocular disparity, precisely superimposed on the surgical field, can facilitate the interpretation of the presented positions and orientations of surgical instruments or models of anatomical structures. The purpose of the current study was to qualitatively assess the OST visualization based on the stereoscopic SPAAM calibration method. The contribution of this study consists in adapting the stereo-SPAAM calibration procedure, developing verification procedures and assessing the accuracy of the spatial visualisation expressed by the error in geometric space representation. This research was conducted for the development of accurate AR visualization methods for CAS. The proposed adaptation of the stereo-SPAAM calibration procedure was implemented in the MentorEye software developed at Wrocław University of Science and Technology (Wrocław, Poland). This project envisages an accurate visualization of AR from the user's perspective, mainly virtual surgery plans (VSP), but also models of anatomical structures or intraoperative imaging data. MentorEye software has been tested in simulated surgical procedures: as a supporting method for fibula free flap harvest and fabrication,15 for mandibular resection [15], and for aiding biopsy procedure [16], AR visualization from the user's perspective has been applied for cutting plane visualization in resection procedures, and to determine the entry point, angle and depth in biopsy procedures.

2. Materials and methods

2.1. Description of participants

The study was conducted on two groups of volunteers: inexperienced users and experienced users. The group of inexperienced users was made up of people who underwent calibration and verification for the first time. The group of experienced users was made up of people who repeated calibration and verification several times. The inexperienced user group consisted of 21 people, while the experienced user group consisted of 5 people. Each participant gave written informed consent to participate in the study.

2.2. The equipment

The tests used an Epson Moverio BT-200 (Seiko Epson Corp., Japan) OST HMD with 960×540 pixel resolution and 23° field of view. An EHDMC10 (Seiko Epson Corp., Japan) wireless mirroring adapter was used to wirelessly send images from a computer to Moverio BT-200. The adapter was connected to the computer with an HDMI cable and used the Miracast standard for wireless connection. A Polaris Spectra (NDI Europe GmbH, Germany) optical navigation system was used for measuring spatial position. A dynamic reference frame consisting of reflective optical markers was mounted to the OST HMD using a previously designed mounting system. Two other reference frames were mounted to display the monitor and skull phantom. A navigated pointed (NDI Europe GmbH, Germany) was used after a prior calibration by the pivoting procedure. The NDI 6D Architect (NDI Europe GmbH, Germany) software was used to define reference frames. Custom-made modules of MentorEye software were used throughout the calibration and verification procedures (described in subsections C and D) as well as during data acquisition. In the experiment, an 18-inch computer monitor was used for calibration and verification. Additionally, a skull phantom with mounted reference frames was used for verification.

2.3. Calibration procedure

A calibration procedure based on the SPAAM method was developed and implemented in the MentorEye software. The proposed calibration procedure was intended for stereoscopic visualization using a binocular OST HMD and involves separate calibrations of the left and right eyes.

The calibration procedure aimed to identify the projection matrix that defines the projection transformation from 3D to 2D coordinate spaces, with elements of this matrix describing the pinhole camera model [4]. The projection matrix was calculated separately for the left and right eyes from 15 pairs of 2D–3D points according to following procedure.

$$M_{3x4} = \begin{bmatrix} g_{11} & g_{12} & g_{13} & g_{14} \\ g_{21} & g_{22} & g_{23} & g_{24} \\ g_{31} & g_{32} & g_{33} & g_{34} \end{bmatrix}. \qquad (1)$$

The indicated pairs of 2D–3D points were separated into two matrices. The P matrix corresponded to

2D points in the HMD layout, while the W matrix corresponded to 3D points.

$$P = \begin{bmatrix} P_{x1} & P_{y1} \\ \vdots & \vdots \\ P_{xn} & P_{yn} \end{bmatrix}, \quad W = \begin{bmatrix} W_{x1} & W_{y1} & W_{z1} \\ \vdots & \vdots & \vdots \\ W_{xn} & W_{yn} & W_{zn} \end{bmatrix}. \quad (2)$$

A matrix equation was then constructed for each pair of points using the previous matrices (Eqs. (2)).

$$\begin{bmatrix} P_{xi} \\ P_{yi} \\ w_i \end{bmatrix} = \begin{bmatrix} g_{11} & g_{12} & g_{13} & g_{14} \\ g_{21} & g_{22} & g_{23} & g_{24} \\ g_{31} & g_{32} & g_{33} & g_{34} \end{bmatrix} * \begin{bmatrix} W_{xi} \\ W_{yi} \\ W_{zi} \\ 1 \end{bmatrix}. \quad (3)$$

After transforming the above matrix equation, the following system of equations was obtained:

$$P_{xi} = g_{11}W_{xi} + g_{12}W_{yi} + g_{13}W_{zi} + g_{14},$$
$$P_{yi} = g_{21}W_{xi} + g_{22}W_{yi} + g_{23}W_{zi} + g_{24}, \quad (4)$$
$$w_i = g_{31}W_{xi} + g_{32}W_{yi} + g_{33}W_{zi} + g_{34}.$$

The P and W matrices were in different units, therefore rescaling was required.

$$x_i = \frac{P_{xi}}{w_i}, \quad y_i = \frac{P_{yi}}{w_i} \quad (5)$$

This allowed the above system of three equations to be written as a system of two equations, thus simplifying the calculations.

$$-x_i(g_{31}W_{xi} + g_{32}W_{yi} + g_{33}W_{zi} + g_{34})$$
$$+(g_{11}W_{xi} + g_{12}W_{yi} + g_{13}W_{zi} + g_{14}) = 0,$$
$$-y_i(g_{31}W_{xi} + g_{32}W_{yi} + g_{33}W_{zi} + g_{34}) \quad (6)$$
$$+(g_{21}W_{xi} + g_{22}W_{yi} + g_{23}W_{zi} + g_{24}) = 0.$$

By performing the transformations presented below, the following matrix was obtained:

$$B * p = 0 \quad (7)$$

where:

$$p = \begin{bmatrix} g_{11} \\ g_{12} \\ g_{13} \\ g_{14} \\ g_{21} \\ g_{22} \\ g_{23} \\ g_{24} \\ g_{31} \\ g_{32} \\ g_{33} \\ g_{34} \end{bmatrix} \quad (9)$$

The final element of the transformation was the determination of the coefficients contained in the p matrix. For this purpose, the matrix was decomposed B using SVD (assuming $\|Bp\|^2$ such that $\|p\| = 1$):

$$B = U * K * V^T \quad (10)$$

The user's task was to align 2D objects (cross-hair) displayed on the OST HMD screen onto an object displayed on an external monitor at a known position in space by moving their head. The spatial position of objects displayed on the computer monitor was known thanks to the earlier mounting of a reference frame on the monitor frame and measuring of the position of the monitor screen in the frame layout with the navigated pointer. The moment the user signalled alignment of the two objects, the position of the object displayed on the monitor was measured relative to the dynamic reference frame mounted on the OST HMD. For each eye, 15 point pairs were collected, five pairs each at three approximate distances of the head from the monitor (approximately 30, 40 and 50 cm). At the end of the procedure, the reprojection error was determined. The calibration procedure is shown in Fig. 1.

$$B = \begin{bmatrix} \vdots & \vdots & \vdots & \vdots & \vdots & \vdots & \vdots & \vdots & \vdots & \vdots & \vdots & \vdots \\ W_{xi} & W_{yi} & W_{zi} & 1 & 0 & 0 & 0 & 0 & -x_iW_{xi} & -x_iW_{yi} & -x_iW_{zi} & -x_i \\ 0 & 0 & 0 & 0 & W_{xi} & W_{yi} & W_{zi} & 1 & -y_iW_{xi} & -y_iW_{yi} & -y_iW_{zi} & -y_i \\ \vdots & \vdots & \vdots & \vdots & \vdots & \vdots & \vdots & \vdots & \vdots & \vdots & \vdots & \vdots \end{bmatrix} \quad (8)$$
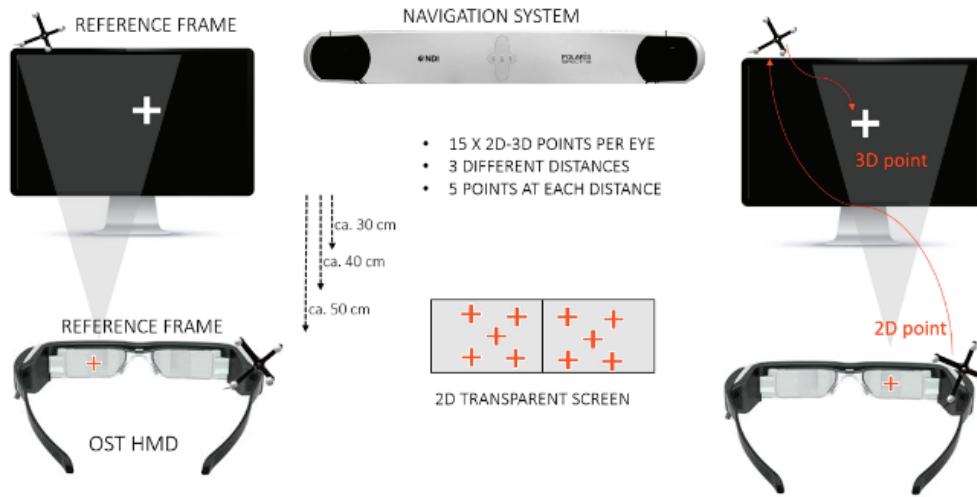
Fig. 1. Experimental setup for calibration procedure

2.4. Validation procedure

The applied validation, presented in Fig. 2, involved the following steps:

- displaying virtual objects in the preset position in 3D space relative to a particular global coordinate system (GCS);
- indicating the perceived position of a visualised point by the user using the navigated pointer;
- calculating the visualization error as the Euclidean distance between the preset position and the indicated, perceived position in the global reference frame.

The validation procedure included three different tests (Fig. 3):
1. 2D visualization test – assessment of the accuracy of visualization of virtual objects arranged on a preset plane,
2. 3D visualization test – the price of accuracy of visualisation of objects arranged in 3D space,
3. Skull phantom validation – assessment of the accuracy of visualisation of objects placed on the surface of a human skull phantom.

The three validation procedures were implemented in custom software, including 3D point visualization on the OST HMD and data acquisition from the navigation system.
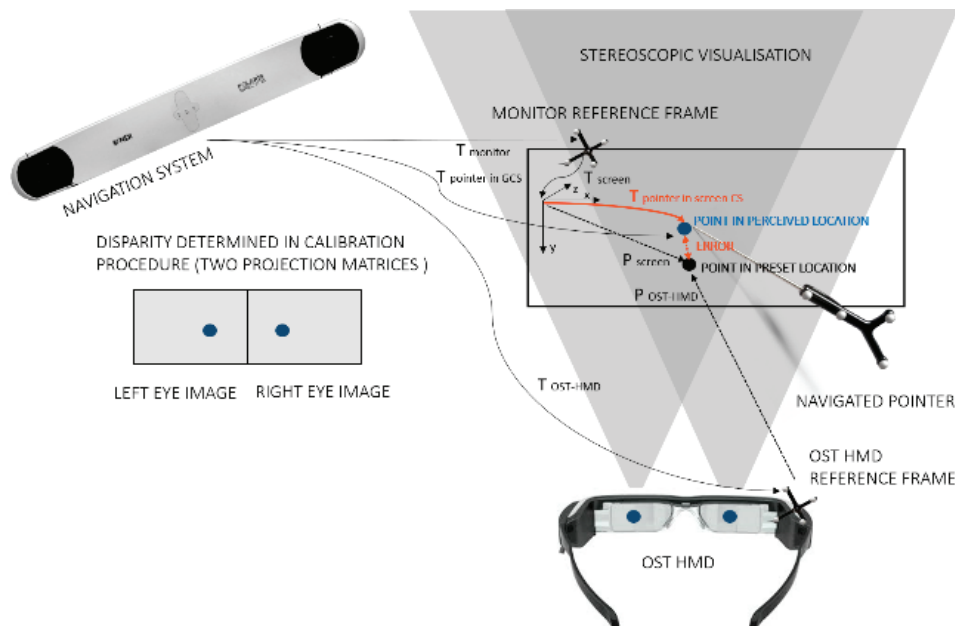

Fig. 2. General validation approach

The coordinates of the preset point were described by the following transformation:

$$T_{\text{OST-HMD}} * T_{\text{Preset}} = T_{\text{monitor}} * T_{\text{Screen}} * T_{\text{Offset}} \quad (11)$$

$$T_{\text{Preset}} = T_{\text{OST-HMD}}^{-1} * T_{\text{monitor}} * T_{\text{Screen}} * T_{\text{Offset}} \quad (12)$$

In the 2D visualisation test, 12 points were displayed in succession on see-through displays of the OST HMD. The points were displayed stereoscopically in a 10×10 cm area, on the plane of the computer monitor screen placed approx. 40 cm from the user. The user was informed that the points were situated on the plane of the screen and, regardless of the perceived depth, always applied the pointer to the surface of screen. The computer monitor was switched off and only provided a background for the test. A reference frame was mounted on the monitor frame and the measurement took place in the coordinate system of the OST HMD screen. The coordinate system of the monitor (Tscreen) was calibrated with the navigator pointer (the screen surface as the XY plane and the Z axis perpendicular to it) relative to the reference frame mounted on the monitor (Tmonitor). The user communicated the alignment of the pointer tip with the visible point by clicking the pen. The operator then recorded the position of the OST HMD, pointer relative to the monitor coordinate system by pressing a button in the application.

In the 3D visualization test, 12 points were displayed at various points in space in front of the monitor in an area of approx. $10 \times 10 \times 3$ cm. The user indicated the position of the perceived point with the pointer tip. In the skull phantom test, 10 points were located on different points on the surface of the skull phantom. The tip of the navigated point was always positioned on the phantom surface, even if the perceived depth was different.

2.5. Data analysis

For each point, 3D distance error (Δ3D) was calculated as geometric distance between its preset position and the position indicated with the tip of navigated pointer. The ΔX, ΔY, and ΔZ coordinate errors were calculated as the distance for each coordinate axis.

For 2D and 3D validation tests, the coordinate system axes were related to the monitor screen plane: X was the horizontal axis, Y was vertical axis, Z is depth axis, and XY was the screen plane). For each person and each of the three tests, the average Δ3D–3D distance error and ΔX, ΔY, and ΔZ coordinate errors were calculated for each point (12 points for the 2D validation test, average of 12 points for the 3D validation test, and average of 10 points for the phantom test). The outliers were then removed based on the box-and-whisker plot (one observation from the 3D validation test for an inexperienced users, one from the 2D test). Finally, error values averaged over all participants were calculated for the inexperienced and experienced
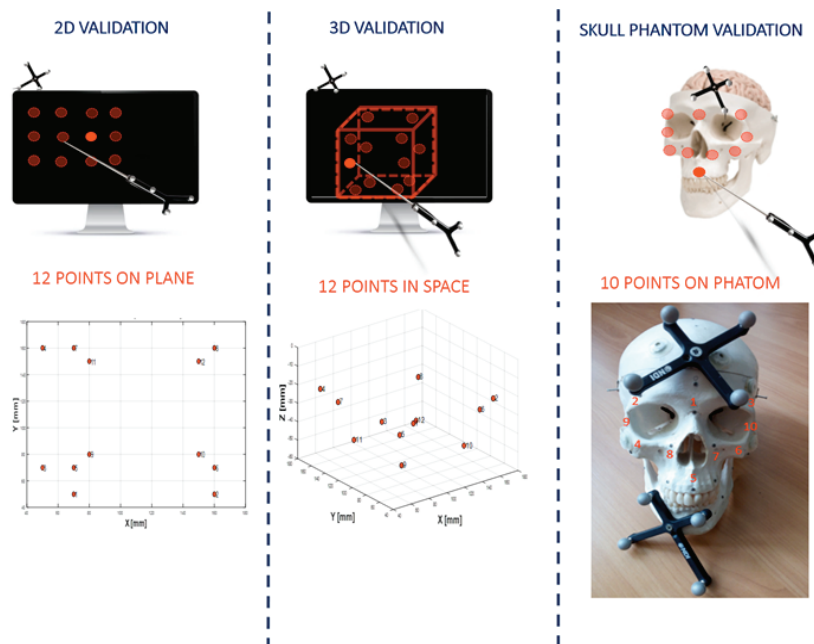

Fig. 3. Three validation tests: 2D validation (12 points located on the plane), 3D validation (12 points located in space), skull phantom validation (10 points located on the skull phantom surface)

users. Wilcoxon signed-rank tests were performed to compare average errors inside the inexperienced group. The threshold of statistical significance was set at $P < 0.05$.

3. Results

In Figure 4, the 3D distance errors (Δ3D) for three different tests: 2D visualisation test, 3D visu-

alisation test and skull phantom visualisation test were compared. The highest visualisation accuracy was obtained for the skull phantom visualisation for an inexperienced users (3.00 mm, std 0.75 mm) and for 2D visualisation test (3.35 mm, std 1.64 mm) for an experienced users. The lowest accuracy was obtained for the 3D visualisation test for an inexperienced users (22.95 mm, std 18.04 mm), and then, also in the case of 3D visualisation, for an experienced users (18.59 mm, std 17.79 mm). The highest accuracy obtained among all users was: Δ3D = 4.64 mm,

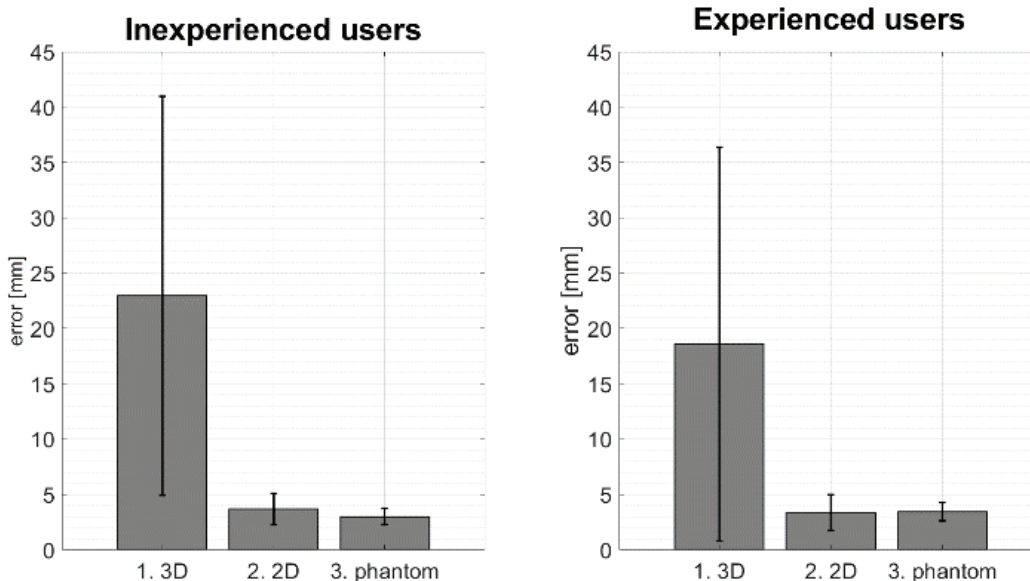Fig. 4. The Δ3D errors for the three tests (3D test, 2D test, skull phantom test)
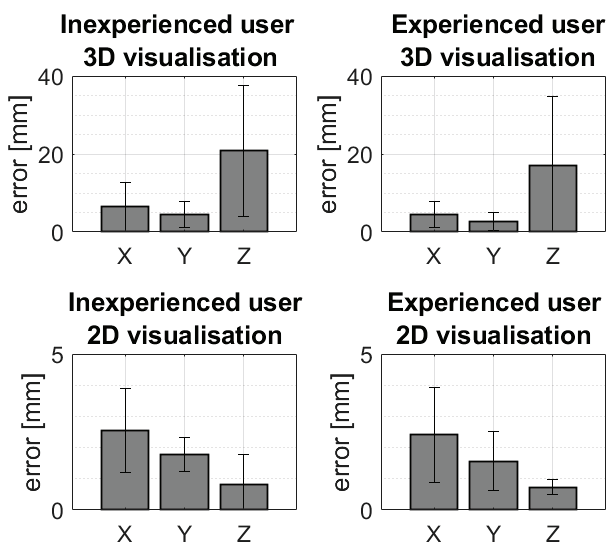for the inexperienced and experienced users

Fig. 5. The Δ*X*, Δ*Y*, and Δ*Z* errors in the horizontal (*X*),
vertical (*Y*), and depth (*Z*) axes for the 3D and 2D tests
for the inexperienced and experienced users

std 2.49 mm (Δ*X* = 1.56 mm, std 1.32 mm; Δ*Y* = 1.11 mm, std 0.69 mm; Δ*Z* = 3.96 mm, std 2.43 mm) for the 3D test and Δ3D = 1.79 mm, std 0.75 mm for the 2D test for the same experienced user and 1.97 mm, std 0.95 mm for the phantom test for an inexperienced user. In Figure 6, the 3D and 2D positions of the measured points and preset points are shown for a single user during the 3D and 2D tests. A user with median 3D error in the 3D test was selected (Δ3D = 12.40 mm, std 13.49 mm for the 3D test and Δ3D = 2.42 mm, std 0.85 mm for the 2D test). The lowest accuracies obtained for the 3D visualisation test suggest that the source of the greatest error was the depth component. An analysis of the Δ*X*, Δ*Y*, and Δ*Z* coordinate errors is presented in Fig. 5. In the case of 3D validation, the *Z* component corresponded to depth, which had the largest error of 20.83 mm, std 16.75 mm for an inexperienced user and 17.13 mm, std 17.50 mm for an experienced user.
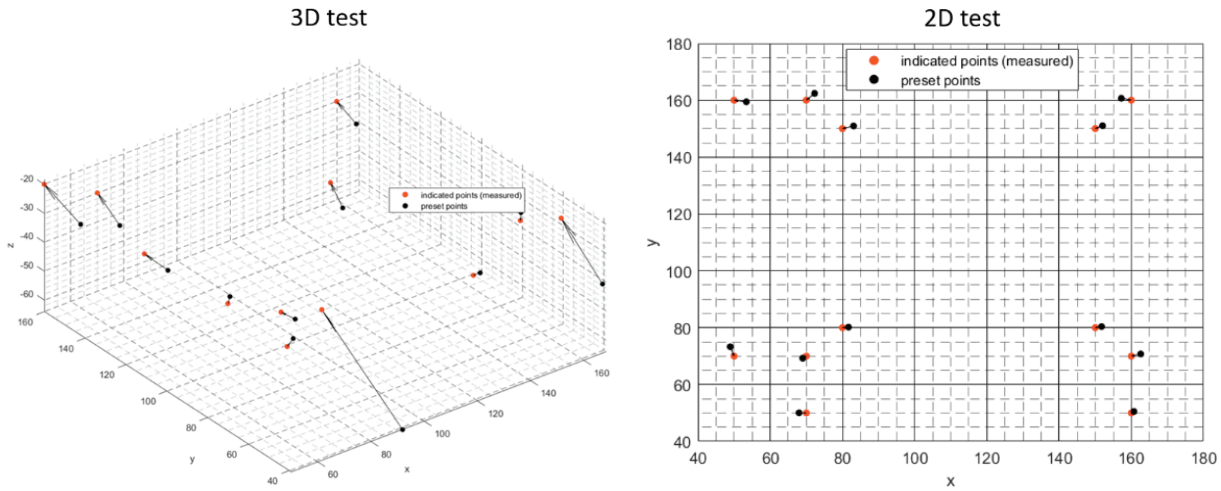
Fig. 6. Positions of the indicated points (measured positions) and preset points during the 3D and 2D tests
for one selected user in the monitor coordinate system (X – horizontal coordinate, Y – vertical coordinate, Z – depth coordinate)

Table 1. P-values obtained
using Wilcoxon signed-rank tests

3D error (Inexperienced users)			
	3D test	2D test	Phantom test
3D test		$P < 0.001$	$P < 0.001$
2D test	$P < 0.001$		0.19
Phantom test	$P < 0.001$	0.19	
3D test (Inexperienced users)			
Symbol	X	Y	Z
X		0.21	$P < 0.001$
Y	0.21		$P < 0.001$
Z	$P < 0.001$	$P < 0.001$	
3D error (Inexperienced users) 3D test vs. 2D test			
	X vs. X	Y vs. Y	Z vs. Z
	$P < 0.01$	$P < 0.001$	$P < 0.001$

4. Discussion

The conducted tests allowed for a qualitative assessment of the accuracy of spatial visualisation of virtual objects displayed on the OST HMD after a prior individual calibration. A proposed variant of the SPAAM method adapted for surgical applications was used for calibration. The proposed variant used an optical navigation system (Polaris Spectra, NDI Europe GmbH, Germany), integrated into surgical navigation systems made by Medtronic, BBraun, and Stryker, used mainly in neurosurgery, orthopaedics, reconstructive surgery and oncological surgery. Surgical navigation systems of other manufacturers usually have integrated optical navigation systems with similar accuracy, sampling rate, and working area. Both calibration (30–40–50 cm) and validation were carried out at eye-to-hand distances and in a working area similar to the working conditions of a surgeon. The results obtained can be translated into surgical applications as well as other similar fields, including in particular manual implementations (e.g., assembly, instruction, quality control, data visualisation in education, training of doctors). Currently, optoelectronic motion tracking systems monitoring the position of active and reflective markers with an accuracy of approx. 0.1–0.2 mm are the gold standard in spatial measurement. The advantages of the SPAAM method are its versatility and ability to be used with various tracking systems. However, it should be noted that the use of a lower accuracy system will affect the accuracy of calibration and accuracy of visualisation. Another source of errors associated with optical navigation systems was the accuracy of calibration of the position of the navigated pointer tip consisting in pivoting the tool around the tip. The pivoting error was less than 0.25 mm. This accuracy affected the indications of the displayed points, but it was also important when transferring coordinate systems to the system of the monitor screen or when defining the position of the points on the phantom skull. A potential source of errors was the movement of the mounted reference frames, including the ones on the OST HMD, monitor screen and phantom. In order to minimise this risk, specially designed and constructed mounting components were used. The accuracy of calibration and validation procedures was also affected by factors such as

involuntary movements of the user's head when overlaying cross-hairs during calibration and involuntary hand shaking when indicating a point or during the confirmation procedure. The influence of these factors was limited by averaging the values for the 20 collected points. The obtained results can be partially related to studies [8]–[10] in which the calibration error was expressed in millimetres. Tang et al. [9] investigated and compared four SPAAM variants: SPAAM, depth-SPAAM, stereo-SPAAM and stylus-mark (Depth-SPAAM using a tracked stylus). The most accurate calibration was obtained for the stylus-marker method, which averaged 23.1 mm, while the worst result was obtained for the SPAAM method, which averaged 69.1 mm. These results were obtained for groups of five to six participants (inexperienced users) per each SPAAM variant. McGarrity et al. [8] tested the planar accuracy of the SPAAM method on a monocular OST HMD. The overall system accuracy averaged over eight participants was 9.3 mm. However, the evaluation did not include stereo-visualisation.

Jun and Kim [10] compared the stereo-SPAAM method to the proposed calibration methods that used a depth camera. The accuracy of the proposed methods was about 2.3 cm while for stereo-SPAAM it varied from about 6 cm to 17 cm depending on the number of points. The accuracy obtained in this study is significantly higher than that of the stereo-SPAAM method implemented by Jun and Kim [10] On the other hand, it is similar to the method using a depth camera. This study also reports the largest error for the depth perception component. The obtained visualization accuracy is similar or higher than that reported by other authors. However, the way the SPAAM method was adapted and the method used to validate its accuracy differ in each of the cited works. This study shows that the main factor introducing the error is the depth component. Displaying objects on a plane perpendicular to the user, but also on curved surfaces, significantly improved the accuracy of the indicated objects, although the visualisation error still remains. Determining the accuracy of visualisation and its repeatability is crucial for the use of AR visualisations in OST HMDs, particularly in surgical applications. The solution to this problem is not relying on visualisation alone but also displaying additional information, such as confirmation that the position and orientation of the navigated tool are within the accepted error margin. This solution was used in the Mentor-Eye software, obtaining surgically acceptable accuracy during simulated resection [15], [18] and biopsy [16] procedures.

5. Conclusion

An adaptation of the stereo-SPAAM calibration was proposed for AR visualisation using an OST HMD together with a quantitative evaluation of the geometric reprojection error. The following visualisation errors were obtained: for 3D points, for the planar test and for the skull test. The errors showed high variability both between users and subsequent measurement points. It seems possible to achieve relatively high visualisation accuracy (of the order of <5 mm for the 3D test and <2 mm for visualisation on the surface) for selected users but ensuring it for the group of inexperienced users seems to be a major challenge. The accuracy obtained depends on human factors relevant to both calibration and validation. The source of the largest error was the depth perception component. A significant improvement in the accuracy of point indication was observed when the points were assumed to be on a plane perpendicular to the user, but also on the skull phantom. In the case of CAS, where AR visualisation is used for precise positioning and orientation of the navigated surgical instruments, the simultaneous presentation of control information may provide the accuracy required in surgery, as demonstrated in previous studies [15], [16], [18].

Acknowledgements

References

[1] AZUMA R., *A survey of augmented reality*, Teleoper. Virtual Environ., 1997, 6 (4), 355–385.

[2] ITOH Y., LANGLOTZ T., SUTTON J., PLOPSKI A., *Towards indistinguishable augmented reality: A survey on optical see-through head-mounted displays*, ACM Comput. Surv., 2021, 54 (6), 1–36.

[3] GRUBERT J., ITOH Y., MOSER K., SWAN J.E., *A survey of calibration methods for optical see-through head-mounted displays*, IEEE Trans. Vis. Comput. Graph., 2018, 24 (9), 2649–2662.

[4] TUCERYAN M., GENC Y., NAVAB N., *Single-point active alignment method (SPAAM) for optical see-through hmd calibration for augmented reality*, Teleoper. Virtual Environ., 2002, 11 (3), 259–276.

[5] GENC Y., TUCERYAN M., NAVAB N., *Practical solutions for calibration of optical see-through devices*, Proc. Int. Symp. Mix. Augment. Real., 2002, 169.

[6] Genc Y., Sauer F., Wenzel F., Tuceryan M., Navab N., *Optical see-through HMD calibration: A stereo method validated with a video see-through system*, Proc. IEEE ACM Int. Symp. Augment. Real., 2000, 165–174.

[7] Zhang Z., Weng D., Liu Y., *A modular calibration framework for 3D interaction system based on optical see-through head-mounted displays in augmented reality*, Int. Conf. Vir. Real. Vis., 2016, 393–400.

[8] McGarrity E., Tuceryan M., Owen C., Genc Y., Navab N., *Evaluation of optical see-through systems*, Proc. Int. Conf. Augment. Virtual Environ. 3D Imag., 2001, 18–21.

[9] Tang A., Zhou J., Owen C., *Evaluation of calibration procedures for optical see-through head-mounted displays*, Proc 2nd IEEE ACM Int. Sym. Mix. Augment. Real., 2003, 161–168, DOI: 10.1109/ISMAR.2003.1240699.

[10] Jun H., Kim G., *A calibration method for optical see-through head-mounted displays with a depth camera*, IEEE Virtual Reality (VR), 2016, 103–111, DOI: 10.1109/VR.2016.7504693.

[11] Moser K., Itoh Y., Oshima K., Swan J.E., Klinker G., Sandor C., *Subjective evaluation of a semi-automatic optical see- through head-mounted display calibration technique*, IEEE Trans. Vis. Comput. Graph., 2015, 21 (4), 491–500.

[12] McGarrity E., Tuceryan M., Owen C., Genc Y., Navab N., *Evaluation of optical see-through systems*, Proc. Int. Conf. Augment. Virtual Environ. 3D Imag., 2001, 18–21.

[13] Venkatesan M., Mohan H., Ryan J.R. et al., *Virtual and augmented reality for biomedical applications*, Cell. Rep. Med., 2021, 2 (7).

[14] Bogdanova R., Boulanger P., Zheng B., *Depth perception of surgeons in minimally invasive surgery*, Surg. Inov., 2016, 23 (5), 515–524, DOI: 10.1177/1553350616639141.

[15] Pietruski P., Majak M., Świątek-Najwer E. et al., *Supporting mandibular resection with intraoperative navigation utilizing augmented reality technology – A proof of concept study*, J. Craniomaxillofac. Surg., 2019, 47 (6), 854–859.

[16] Majak M., Żuk M., Świątek-Najwer E., Popek M., Pietruski P., *Augmented reality visualization for aiding biopsy procedure according to computed tomography based virtual plan*, Acta Bioeng. Biomech., 2021, 23 (2), 81–89.

[17] McGarrity E., Genc Y., Tuceryan M., Owen C., Navab N., *A new system for online quantitative evaluation of optical see-through augmentation*, Proc. IEEE ACM Int. Symp. Augment Real., 2001a, 157–166.

[18] Pietruski P., Majak M., Świątek-Najwer E. et al., *Supporting fibula free flap harvest with augmented reality: A proof of concept study*, Laryngoscope, 2020, 130 (5), 1173–1179.